

Received: 2017.02.19  
Accepted: 2017.03.27  
Published: 2017.10.04

# Effect of Fibronectin-Coated Micro-Grooved Titanium Surface on Alignment, Adhesion, and Proliferation of Human Gingival Fibroblasts

Authors' Contribution:  
Study Design A  
Data Collection B  
Statistical Analysis C  
Data Interpretation D  
Manuscript Preparation E  
Literature Search F  
Funds Collection G

ABCE 1 **Xiaochong Jian**  
B 2 **Wenxiu Huang**  
C 2 **Dong Wu**  
F 2 **Dongdong You**  
B 1 **Zhaonan Lin**  
AG 2 **Jiang Chen**

1 School of Stomatology, Fujian Medical University, Fuzhou, Fujian, P.R. China  
2 Department of Oral Implantology, Fujian Stomatological Hospital, Affiliated Hospital of Fujian Medical University, Fuzhou, Fujian, P.R. China

**Corresponding Author:** Jiang Chen, e-mail: [dentistjiang@126.com](mailto:dentistjiang@126.com)  
**Source of support:** Departmental sources

**Background:** Surface characters of culture plates affect cellular behaviors such as cellular alignment and elongation. Microgrooves guide the cell growth along the grooves and spread. The aim of this study was to observe the effect of fibronectin (FN)-coated micro-grooved titanium plates on the alignment, spread, adhesion, and proliferation of human gingival fibroblasts (HGFs).





**Material/Methods:** Micro-grooved titanium plates were fabricated, and FN was immobilized onto the micro-grooved surfaces using silanization. HGFs were cultured on the smoothed or micro-grooved (with 35 μm width, 15 μm bridge, 10 μm depth) titanium plates, with or without the FN coating. We assessed the water contact angle and blood compatibility of the surfaces, and the earlier adhesion, adhesion strength, proliferation and morphology of the cells growing on the different titanium surfaces.

**Results:** The results revealed that the blood hemolysis rates of different titanium surfaces were within the safety limits. HGFs aligned along the grooves, spread out more evidently, and showed significantly more adhesion in the FN-coated micro-grooved surface compared with other surfaces ( $p < 0.05$ ).

**Conclusions:** The micro-grooved surface coated with FN guides the HGFs to align along the grooves, and promotes cell spread, adhesion and proliferation, which might be used to improve the efficacy of dental implants.

**MeSH Keywords:** **Fibroblasts • Fibronectins • Titanium**

**Full-text PDF:** <https://www.medscimonit.com/abstract/index/idArt/903883>

 4039  4  11  19



## Background

Titanium has been practically employed as a reliable biomaterial for dental implants to treat edentulous areas. Peri-implant soft tissue is vulnerable to bacterial invasion that may cause peri-implant disease [1]; therefore, the key to the success of dental implantation is the constitution of a soft tissue barrier able to promote osseointegration surrounding the implant body [2]. Learning how to form firm and functional soft tissue sealing around the titanium implant is particularly important.

Neck surface characteristics of dental implants, such as surface microtopography, influence the implant soft tissue interface [3]. It was reported that the micro-grooved structure effectively induced the formation of the vertical direction of the collagen fiber secreted by cells, guided the cell alignment and elongation along the microgroove, limited the epithelial cell downward growth, and decreased the occurrence of inflammation around implants [4,5]. Compared with smoothed titanium, micro-grooved titanium substrata promoted the adhesion and proliferation of HGFs as well as adhesion to peri-implant soft tissue [1,6,7].

Fibronectin (FN), an important extracellular matrix molecular, promotes the adhesion of cells to matrix [8], which is strictly related to the focal adhesion via its Arg-Gly-Asp-Ser sequence that binds integrins. It was demonstrated that the FN-conjugated micro-grooved titanium substrate promoted the osteoblast differentiation of human bone marrow-derived mesenchymal stem cells [9]. Another report showed that compared with the microgrooves without coating, the FN-coated microgrooves increased the area of Hela cell spreading but significantly decreased the percentage of aligned cells [10]. However, the effect of FN-coated micro-grooved titanium substrate on the behaviors of human gingival fibroblasts (HGFs) has not been reported yet.

The aim of this study was to evaluate the effect of FN-immobilized micro-grooved titanium surface on the alignment, spread, adhesion, and proliferation of HGFs.

## Material and Methods

### Titanium plates

Titanium plates (99.9% purity, ASTM GR.1) 1 mm thick and 10 mm in diameter were purchased from Baoji INT Titanium Material Co., Ltd. (Baoji, China). The titanium plates were polished by using waterproof abrasive paper (type 200 #, 600 #, 800 #, 1000 #, and 1500 #). Microgrooves were obtained by a numerically controlled tool. The roughness (expressed as average roughness values, Sa) and dimensions of the surface

patterns were measured by an OLS4100 3D laser microscope (Olympus, Tokyo, Japan).

### Salinization of titanium

The titanium plates were successively ultrasonicated for 15 min in acetone, alcohol, and distilled water. The cleaned plates were activated in 5 M NaOH at 60°C for 30 min and then cleaned with deionized water. The activated plates were salinized by submerging in 2% (3-aminopropyl) triethoxysilane (APTES) for 4 h and then heated at 100°C to film for 1 h. After that, all plates were sterilized in ethanol for 2 h, washed with distilled water 3 times, and dried before use. The composition of element C, O, N, Ti, and Si in titanium plates was detected by an X-ray photoelectron spectroscopy (XPS, ESCALAB 250, Thermo Scientific, Waltham, MA, USA). The purity of the titanium of plates was evaluated by the assessment of the impurities (including chromium, sodium, and vanadium impurities) using an Energy Disperse Spectroscopy (EDS) of Nova NanoSEM 230 field emission scanning electron microscopy (FEI, Hillsboro, OR, USA).

### Conjugation of FN with titanium plates

FN solution was diluted to 25, 50, 100, 200, 300, and 400 µg/ml, and the silanized titanium materials were soaked in various concentrations of FN solution for 4 h. After the conjugation, 25 µl of solution was then taken to measure the protein concentration according to the protocol of the manufacturer's kit by using BCA reagents (Cat#P0012, Beyotime Biotech., Shanghai, China). The conjugation capacity of FN with titanium was calculated by the equation:  $AQ = M - (C1 - C2) V$ , where AQ denoted the amount of adsorbed protein (mg), M was for the initial amount of protein solution (mg), C1 for the initial protein concentration (mg/ml), C2 for the protein concentration after the conjugation (mg/ml), and V for FN solution volume (ml).

### Titanium surface characterization

The covalent conjugation of FN with the micro-grooved titanium surface was determined by XPS with an ALKα X-ray source (1468.6 eV). The surface morphologies of different surfaces were characterized with an environmental scanning electron microscope (ESEM, XL30 ESEM-TMP, Philips-FEI, Holland). The roughness of different surfaces was measured by a 3D OLS4100 laser microscope. Water contact angles (θc) were measured by an auto-contact angle analyzer (Phoenix 300, Surface Electros Optics, Suwon, Korea).

### Blood compatibility

The hemolysis rate (HR) test is commonly used to assess the blood compatibility of biomaterials. Human peripheral blood

was collected from healthy volunteers in accordance with the protocols approved by the Ethics Committee of Affiliated Stomatological Hospital of Fujian Medical University (Fuzhou, China). Human blood was anticoagulated by adding 3.8% sodium citrate solution at a ratio of 9: 1 (vol/vol) and diluted by sodium chloride solution at a ratio of 4: 5 (vol/vol). Two hundred  $\mu\text{L}$  of diluted anticoagulated human blood was added to FN-coated smoothed titanium plates (S+FN) treated with 10 ml 0.9% NaCl, FN-coated micro-grooved plates (G+FN) treated with 10 ml 0.9% NaCl, positive control treated with 10 ml distilled water, and negative control treated with 10 ml 0.9% NaCl. The samples were incubated at 37°C for 60 min, and then centrifuged at 3000 rpm for 5 min. The supernatant was collected and we measured the optical absorbance at 545 nm using a microplate reader (Humareader, HUMAN GmbH, Germany) to assess the content of free hemoglobin. The HR of the samples was calculated using the following formula:  $\text{HR} = (\text{Dt} - \text{Dnc} / \text{Dpc} - \text{Dnc}) \times 100\%$ , where Dpc and Dnc denoted the absorbance of the positive and negative controls at 545 nm, respectively, and Dt denoted the absorbance value of samples. The experiments were repeated 6 times.

### Cell culture

Human gingival fibroblasts (HGFs) were isolated from healthy gingival tissues of orthodontic patients who had their pre-molar teeth removed. The procedure was approved by the Ethics Committee of the Affiliated Stomatological Hospital of Fujian Medical University. Gingival tissues were minced to debris of about 3 mm<sup>3</sup>, placed in 6-well plates, covered by a cover slip to prevent debris from floating, and maintained in Dulbecco's modified Eagle's medium (GIBCO, Carlsbad, CA, USA) supplemented with 10% fetal bovine serum (Hyclone, Logan, UT, USA) and 1% (v/v) penicillin-streptomycin solution (Hyclone) at 37°C in 5% CO<sub>2</sub> in an incubator. The growth medium was changed every 2–3 days, and cells were sub-cultured when they reached 80–90% confluence. Cells at passages 3–5 were used in the following experiments.

### Cell morphology

HGFs were seeded onto different titanium culture plates at a density of  $1 \times 10^4$  cells/well, which were placed into 6-well plates, with 1 plate in 1 well. After 3 days of culture, the titanium plates were gently rinsed with phosphate-buffered saline (PBS) and moved to new 6-well plates. The cells on the titanium plates were fixed with 4% glutaraldehyde for 2 h and then washed twice with PBS. Subsequently, the cells were dehydrated with a series of ethanol solutions (30%, 50%, 70%, 90%, and 100%), subject to critical-point drying and platinum-coating, and were finally observed under a Nova NanoSEM 230 scanning electron microscope (SEM, FEI).

### Cell early adhesion

The adhesion of HGFs to S, G, S+FN, and G+FN titanium plates was detected by 4,6-diamidino-2-phenylindole (DAPI) fluorescence staining [11,12]. HGFs were seeded on the titanium plates at a density of  $5 \times 10^4$  cells/plate in 6-well plates. After being cultured for 2 h, 4 h, and 6 h, respectively, cells were detached from the plates with 500  $\mu\text{l}$  trypsin-EDTA for 5 min, rinsed with PBS 3 times, and added to 500  $\mu\text{l}$  fresh culture medium. After centrifugation, 1 ml culture medium was added, and cell suspension on the titanium plates was transferred to new 6-well plates. Cells detached were counted with a Coulter Z1 device (Coultronics, Margency, France). Experiments were repeated 3 times and the average value was taken.

### Cell adhesion strength

Cells were plated on the titanium plates at the density of  $5 \times 10^4$  cells/plate in 6-well plates. After culturing for 2 h, 4 h, 8 h, 12 h, and 16 h, cell samples were enzymatically detached from the titanium plates by diluted trypsin-EDTA [0.025% (v/v)] treatment for 10, 30, and 60 min. The remaining adherent cells were further detached by 15-min treatment in 0.25% undiluted trypsin-EDTA. Cells detached were counted with a Coulter Z1 device. The curve of the percentages of the released cells versus tyrosination time was drawn. The area projected by the curve on the X-axis (denoting enzymatic time) was evaluated by integration, which was considered as the cell detachment index (D(t)) inversely proportional to the cell adhesion on the biomaterial [11,13]. Experiments were repeated 6 times and the average value was taken.

### Cell proliferation

HGFs ( $1 \times 10^4$ ) were seeded onto the different titanium plates and cultured for 1 d, 3 d, 5 d, and 7 d, respectively. The growth medium was changed every 2–3 days. After each culture period, the cells on the titanium plates were washed with PBS, moved to new 6-well plates, added to 500  $\mu\text{l}$  fresh culture medium and 50  $\mu\text{l}$  CCK-8 solution (Dojindo, Japan), and incubated at 37°C for another 2 h. The optical absorbance at a wavelength of 450 nm was measured with a microplate reader. The viability of cells was determined according to the protocol of the kit.

### Immunofluorescence staining

HGFs were seeded onto different titanium plates at a density of  $1 \times 10^4$  cells/well in 6-well plates. After culturing for 3 days, the cells were gently rinsed with PBS and moved to new 6-well plates. Cells were fixed with 4% paraformaldehyde for 10 min, permeabilized in 0.5% TritonX-100 (T8787, Ronkonkoma, NY, Sigma, USA) for 5 min, and then blocked with 1% bovine serum albumin for 30 min. We then added 300  $\mu\text{l}$  of mouse

**Table 1.** Roughness of titanium surfaces (n=5).

Waterproof abrasive paper	Sa (µm)
600#	0.331±0.022
800#	0.283±0.046
1000#	0.218±0.053
1500#	0.178±0.017

**Table 2.** Designed and measured actual parameters of microgrooved titanium surfaces.

	Designed	Actual
Groove width (µm)	35.00	36.67
Groove depth (µm)	15.00	14.52
Ridge width (µm)	10.00	9.43

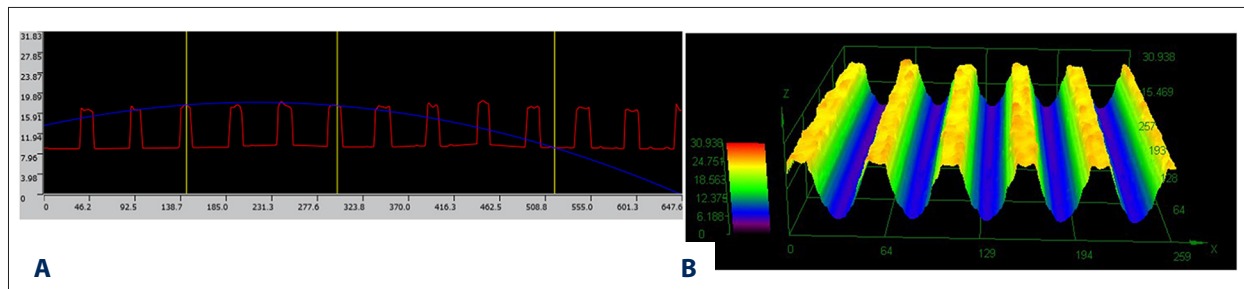


**Figure 1.** Surface texture dimensions of titanium plates observed by 3D laser scanning microscope. (A) 3D laser scanning microscopic observation of the plan of the micro-grooved titanium plate (1000x); (B) 3D laser scanning microscopic observation of the 3D figure of the micro-grooved titanium plate (1000x).

anti-vinculin monoclonal antibody (1: 200, V9131, Sigma) into each well and incubated them at 37°C for 1 h. After washing with PBS, the cell samples were stained with anti-mouse FITC-conjugated IgG (whole molecule) (1: 32, F0257, Sigma) for 30 min at room temperature in the dark. Subsequently, the cell samples were stained with rhodanine phalloidin (1: 400, Cat. # PHDR1, Cytoskeleton, Denver, CO, USA) for 30 min in the dark, and then stained with DAPI (1: 1000, D9542, Sigma) for 5 min. Finally, the samples were sealed with mounting reagent (S3023, DAKO, Shanghai, China) and observed under a laser scanning confocal microscope (LSM710, Carl Zeiss Microscopy, GmbH, Germany). Images were processed using Microsoft Image Pro Plus 5.0 software.

**Bacterial adhesion**

*P. gingivalis* was purchased from the American Type Culture Collection (ATCC 33277, Manassas, VA, USA). *P. gingivalis* was cultured in brain heart infusion broth (BHI)-blood agar plates at 37°C under anaerobic conditions (10% CO<sub>2</sub>, 10% H<sub>2</sub>, and 80% N<sub>2</sub>). A single colony of *P. gingivalis* strain was selected from the BHI-blood agar plates and then incubated in broth at 37°C anaerobically for another 6 h to reach logarithmic phase growth. Then, *P. gingivalis* suspension was diluted to 1×10<sup>6</sup> colony-forming units (CFUs)/ml, which corresponded to 0.1 unit of optical absorbance at 600 nm. One hundred µl of suspension was seeded onto each titanium disc and incubated in 12-well culture plates at 37°C for 2 h. Then, titanium discs were washed twice with PBS and resuspended in Ringer’s buffer to detach bacteria by vortexing vigorously. The bacteria were collected,

diluted 100-fold, and plated on BHI-blood agar plates. After 2 days of anaerobic incubation at 37°C, the CFUs on the plates were manually counted.

**Statistical analysis**

The data were expressed as the mean values ± standard deviation and were compared between different groups at each time point using one-way analysis of variance followed by the post hoc LSD test. P<0.05 was considered significant.

**Results**

**Titanium surface characterization**

3D laser microscopic observation showed that after the polishing with waterproof abrasive paper 1500#, the Sa value was 0.178 µm. The titanium plates were polished under this condition to mimic the surfaces of the transgingival areas of commercially available titanium dental implant abutments whose Sa was nearly 0.20 µm. The titanium surface roughness, actual parameters, and surface texture dimensions are shown in Tables 1 and 2, and Figure 1, respectively. In addition, EDS examination showed no chromium, sodium, or vanadium impurities in the titanium surfaces (Figure 2).

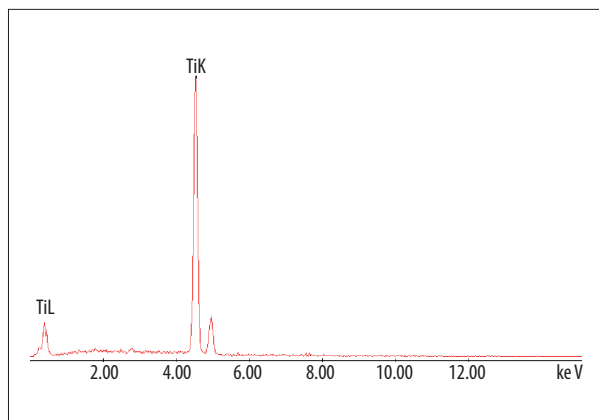


**Figure 2.** EDS examination of the titanium plate surface.

### Surface modification and characterization

XPS examination showed there were 4 elements – Ti, C, O, and N – in the pristine micro-grooved titanium surfaces (Figure 3). Particularly, element Si was detected only after the silanization (Table 3), which indicated the success of silanization. The increase of elements N and C and reduction of O, Ti, and Si after the immobilization of the FN (Table 3) suggested the modification role of FN in the titanium material. XPS examination revealed the same surface modification and characterization in the smoothed titanium surfaces (unpublished data), showing that the surface microtopography had no obvious effect on the conjugation of FN with the titanium surfaces.

SEM observation showed that after the silanization, the microgroove structure still existed and the size was unchanged, but a porous network gel layer was observed on the surface (Figure 4). 3D laser microscopic observation showed that after the alkali and heat treatment, the roughness ( $S_a$ ) of the smoothed titanium surface was obviously decreased, while that of the micro-grooved titanium surface remained almost unchanged (Table 4).

The hydrophilicity of the different surfaces was detected by determining the water contact angle. Table 4 shows that after the silanization, the water contact angles in the smoothed and grooved titanium surfaces were significantly increased from pretreatment ( $60.71 \pm 3.87$  and  $40.92 \pm 2.64$ , respectively) to

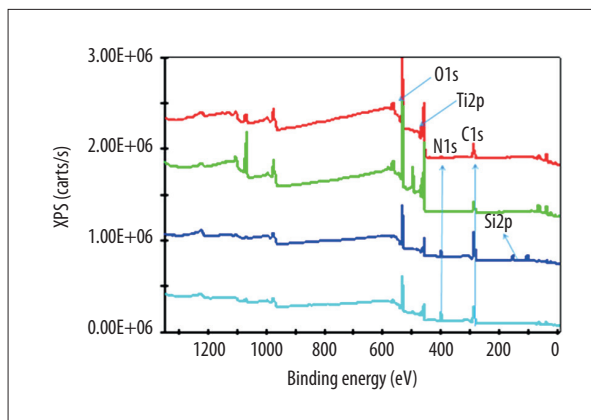


**Figure 3.** Surface texture dimensions of titanium plates observed by 3D laser scanning microscope. 3D laser scanning microscopic observation of the plan of the microgrooved titanium plate (1000 $\times$ ).

$94.92 \pm 4.31$  and  $91.24 \pm 4.94$ , respectively, indicating that etching with alkali made the surface more hydrophilic. In addition, after the immobilization of FN, the water contact angles were decreased slightly but were still higher than the treatment (Table 4).

### Conjugation of FN with titanium surfaces

Figure 5 shows that FN conjugated with titanium surfaces in a dose-dependent manner until the concentration of FN reached 300  $\mu\text{g/ml}$ . Therefore, 300  $\mu\text{g/ml}$  of FN was used to conjugate with the titanium surfaces in the following experiments.

### Hemolysis rate

Since artificial materials implanted into the human body interact with the red blood cells, which would cause hemolysis, HR of titanium plates was assessed. The result showed HR of the smoothed titanium, micro-grooved titanium, FN-conjugated smoothed titanium, and FN-conjugated micro-grooved titanium was  $0.469 \pm 0.016$ ,  $0.469 \pm 0.078$ ,  $0.328 \pm 0.033$ , and  $0.453 \pm 0.022$ , respectively, which was within the prescribed scope of safe use ( $< 5\%$ )

**Table 3.** Effects of silanization on the percentage of element C, O, N, Ti and Si of titanium surfaces.

Sample	%C	%O	%Ti	%N	%Si
Ti	32.68	51.38	12.16	3.78	
Ti+NaOH	22.51	54.42	21.99	1.08	
Ti+NaOH+APTES	47.35	39.35	9.97	8.79	4.54
Ti+NaOH+APTES+FN	49.02	27.40	7.41	15.19	0.98

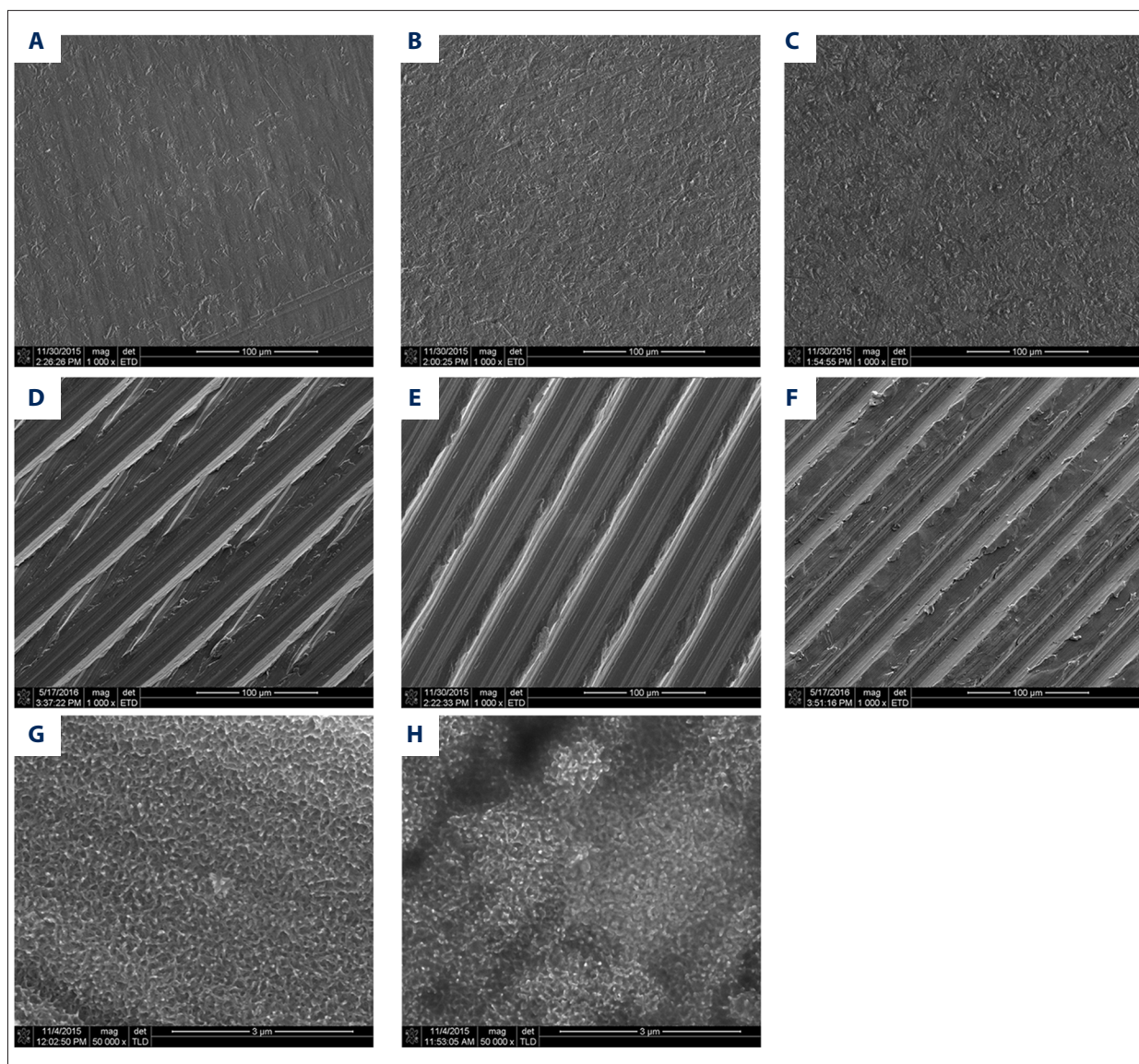


**Figure 4.** The characteristics of different titanium surfaces. (A–F) SEM observation of smoothed titanium (S) and micro-grooved titanium (G) surfaces at 1000 $\times$ , with the bar length corresponding to 100  $\mu\text{m}$ . (A) Smoothed titanium surface; (B) Smoothed titanium surface + NaOH; (C) Smoothed titanium surface + NaOH+(3-aminopropyl) triethoxysilane (APTES); (D) Micro-grooved titanium surface; (E) Micro-grooved titanium surface + NaOH; (F) Micro-grooved titanium surface + NaOH + APTES. (G, H) SEM observation of micro-grooved titanium surface subject to alkali (G, titanium + NaOH) and silanization (H, titanium + NaOH+ APTES) treatment at 50 000 $\times$ , with the scale bar length corresponding to 3  $\mu\text{m}$ .

### Cell early adhesion

Figure 6 shows that the number of cells that adhered to various titanium plates increased with time. The numbers of cells adhered to FN-coated smoothed plates (S+FN group) were the highest at 2 and 4 h. However, at 6 h there was no significant difference in the numbers of adhered cells between all types of titanium plates ( $P>0.05$ ).

### Cell adhesion strength

As shown in Figure 7, Dt of S, G, S+FN, and G+FN plates was decreased in sequence, indicating that cell adhesion strength was increased from S, G, S+FN, to G+FN titanium plates in turn. Particularly, cell adhesion strength of G+FN plate was the strongest, and reached a peak at 6 h, which was earlier than that of other plates.

**Table 4.** Roughness and water contact angel of titanium surfaces (n=5).

		Sa	Water contact angel (θc)
S	Ti	0.178±0.006	60.71±3.87
	Ti+NaOH	0.183±0.005	27.82±1.43
	Ti+NaOH+APTES	0.047±0.003	94.92±4.31
	Ti+NaOH+APTES+FN	0.049±0.002	83.97±4.18
G	Ti	1.086±0.017	40.92±2.64
	Ti+NaOH	1.095±0.015	18.04±1.57
	Ti+NaOH+APTES	1.042±0.019	91.24±4.94
	Ti+NaOH+APTES+FN	1.081±0.025	74.73±4.82

Sa – average roughness values; Ti – titanium; APTES – (3-aminopropyl)triethoxysilane; FN – fibronectin.

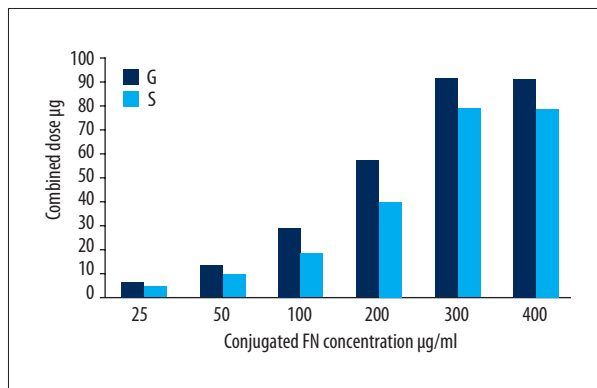


**Figure 5.** Dose-dependent FN conjugation with titanium plates.

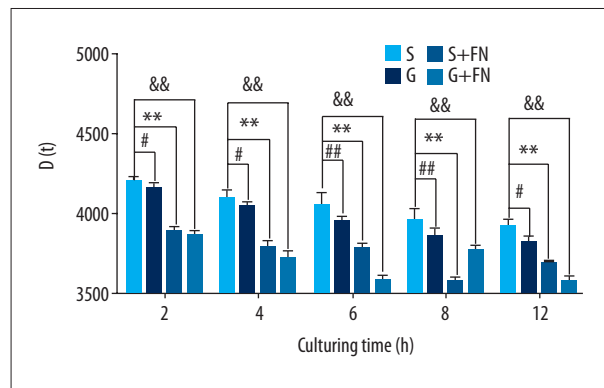


**Figure 7.** Cell adhesion strength of the different titanium plates. # P<0.05, ## P<0.01 G group compared with S group, \*\* P<0.01 S+FN group compared with S group, & P<0.05, && P<0.01 G+FN group compared with S group.

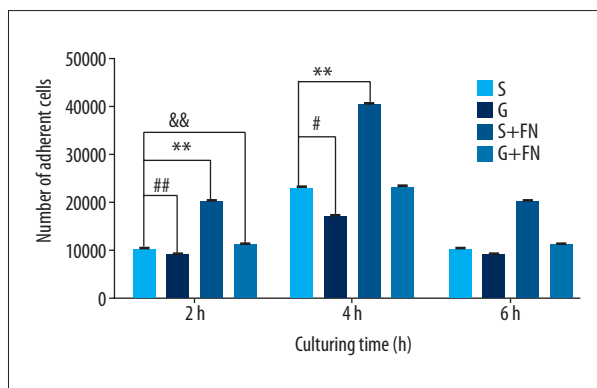


**Figure 6.** Earlier cell adhesion of the different titanium plates. # P<0.05, ## P<0.01 G group compared with S group, \*\* P<0.01 compared with S+FN group S group, && P<0.01 G+FN group compared with S group.

### Cell morphology and spreading

On smoothed plates, cells looked flat, most of which were polygon-shaped, without consistent orientation, but on micro-grooved titanium plates the HGFs presented an elongated shape and were aligned along the groove direction, maintaining

a semi-flattened shape (Figure 8). Cells cultured on S+FN plates looked more spread out compared with cells on S plates. Cells on G+FN plates were more spread out and formed a confluent cell layer covering almost the whole surface, including the bottom, at 3 days, compared with cells along the side wall, which bridged the grooves instead of adhering directly onto the bottom on the micro-grooved plates (Figure 8).

### Cell proliferation

As shown in Figure 9, after 2 days of culturing, there were more living cells on the G and G+FN titanium plates compared with S plates. At 3 and 4 days, cells on G and G+FN plates, were significantly more numerous than cells on S and S+FN plates (P<0.05). Interestingly, cells on G+FN and S+FN plates were significantly less numerous than cells on G and S plates (P<0.05).

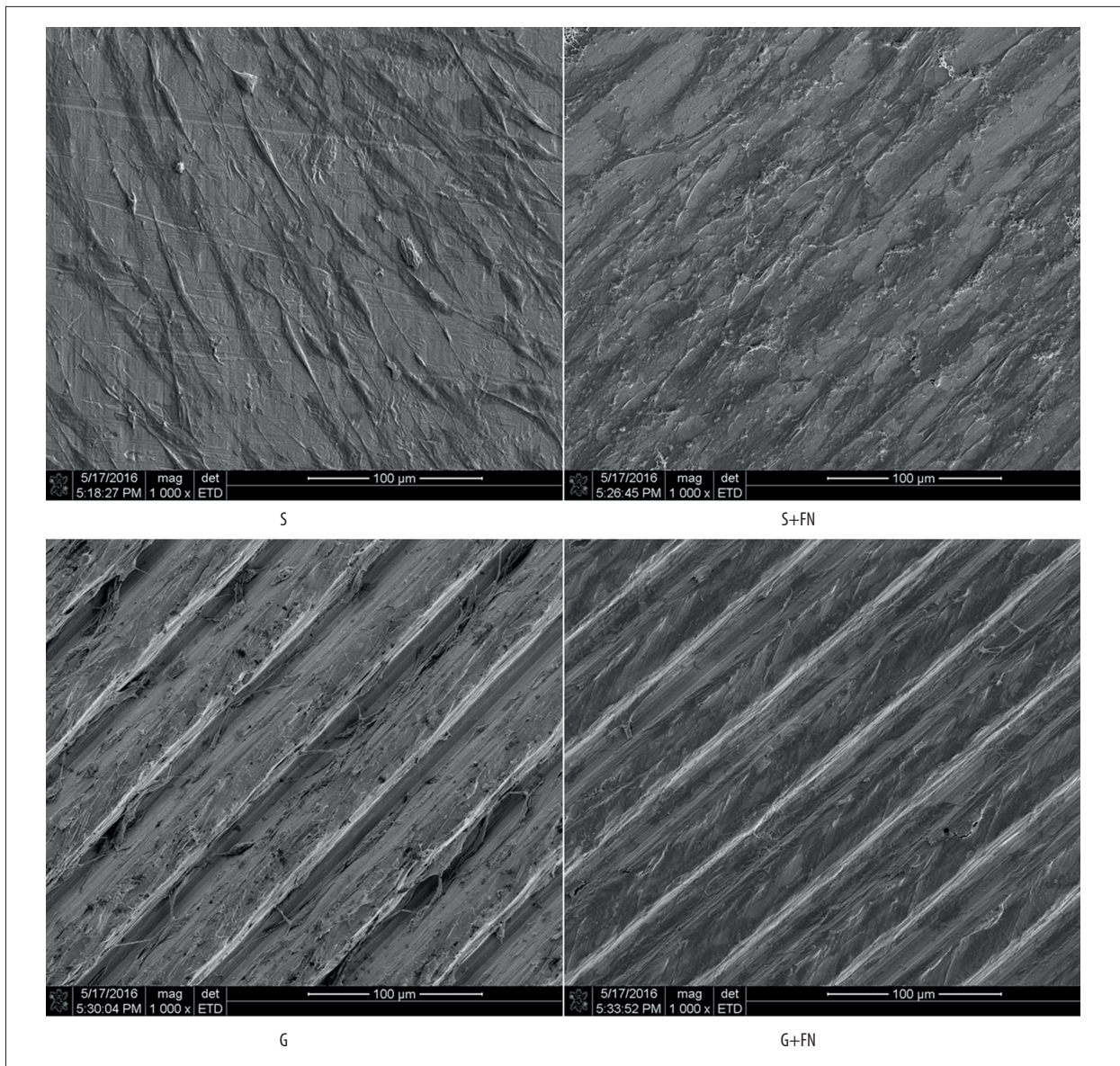
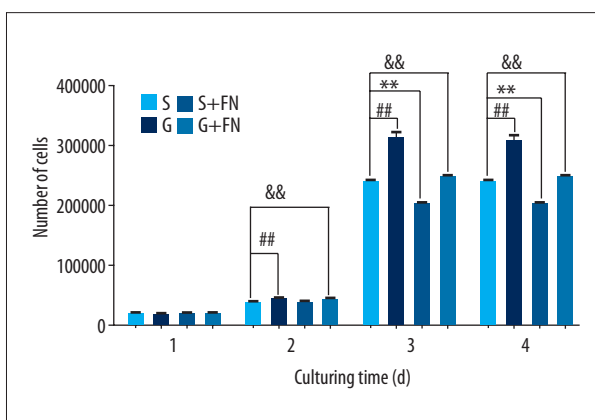


Figure 8. Morphology of HGFs on different titanium plates (×1000).



**Immunofluorescence staining**

To further observe the orientation, morphology, and cytoskeleton of HGFs on different titanium plates, cells were immunostained with vinculin. We found that the cells grown on S and S+FN plates had no clear orientation (Figure 10). In contrast, the cells cultured on G and G+FN plates had a specific orientation, aligning along the grooves, and grew inside the

Figure 9. Proliferation of HGFs on different titanium plates. ## P<0.01 G group compared with S group, \*\* P<0.01 S+FN group compared with S group, && P<0.01 G+FN group compared with S group.



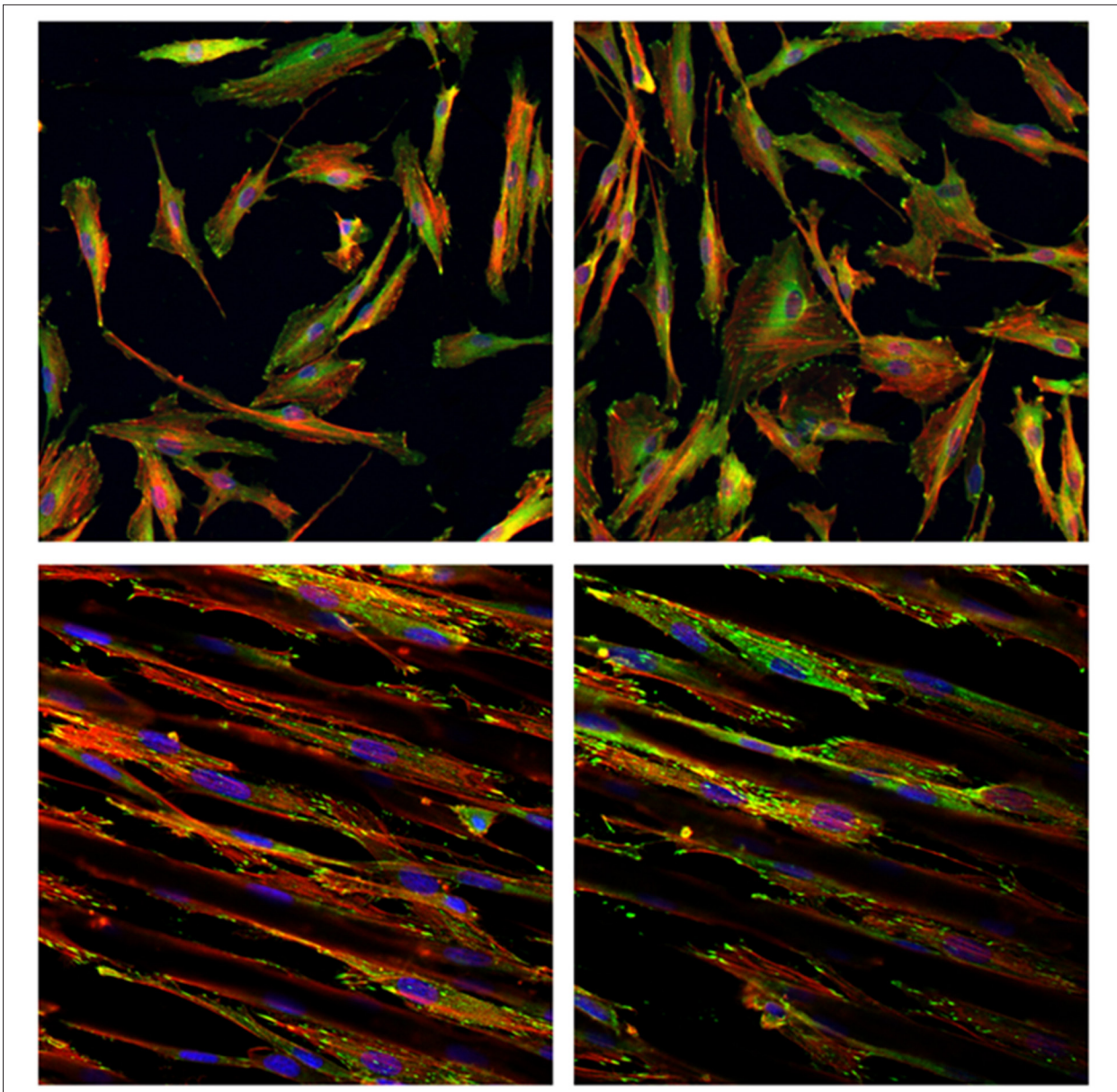


**Figure 10.** Immunofluorescence staining of HGFs on different titanium plates. The green dot denotes the expression of vinculin protein, the red shows rhodanine-stained cytoskeleton, and the blue shows DAPI-stained nuclei (200×).

microgrooves, on the ridge, or on both of them (Figure 10). In addition, compared with S or G plates, HGFs on S+FN and G+FN plates showed higher expression of vinculin, indicating more cytoskeleton in these cells.

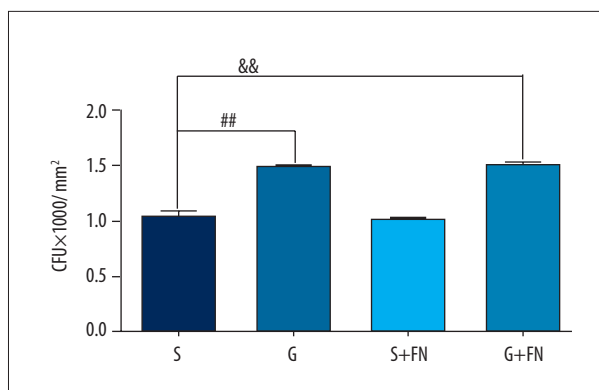
#### Bacterial adhesion

Figure 11 shows that the adhesion of *P. gingivalis* was significantly enhanced on G and G+FN titanium plates compared with S plates ( $p < 0.01$ ), but there was no difference between S and S+FN plates ( $p > 0.05$ ).

#### Discussion

The effect of FN-coated micro-grooved titanium substrate on the behaviors of HGFs has not been reported previously. In the present study, modified titanium substrates with microgroove were fabricated and conjugated with FN. We showed that FN-conjugated micro-grooved titanium substrates supported the cell orientation along the grooves, as well as spread, adhesion, and proliferation of HGFs.

Thirty  $\mu\text{m}$  roughly represents the diameter of fibroblasts [14]. Microgrooves with the width of 30  $\mu\text{m}$  enables HGFs to readily



**Figure 11.** Bacterial adhesion with different titanium plates.  
##  $P < 0.01$  G group compared with S group, &&  $P < 0.01$  G+FN group compared with S group.

descend into the grooves and promotes cell proliferation [14]. Titanium substrata with a bit wider grooves (e.g., 35  $\mu\text{m}$ ) supported more cells compared with narrower grooves [15]. Consistently, the microgrooves with width of about 35  $\mu\text{m}$  in this study effectively guided the HGFs into the bottom of the grooves. It was reported that groove depth influences the alignment and elongation of epithelial cells on micro-grooved plates [5]. As to the depth of grooves, when the width was fixed, contact guidance was increased with the groove depth (from 1  $\mu\text{m}$  and 5  $\mu\text{m}$  to 10  $\mu\text{m}$ ) [16]. Therefore, in the present study, we selected the micro-grooved titanium plates with 35  $\mu\text{m}$  width, 15  $\mu\text{m}$  bridge, and 10  $\mu\text{m}$  depth.

FN promotes the adhesion of cells to matrix [8], which is beneficial for dental implantation. However, due to competition from other serum proteins or physical abrasion, FN might be desorbed from the implants *in vivo*. To overcome any possible desorption, the silanization method was used to covalently bond FN to titanium. As to the immobilized dose of FN, we showed that the immobilization of FN increased with the concentration of FN solution until the latter reached 300  $\mu\text{g}/\text{ml}$ . Silane's  $\text{NH}_2$  group number on the titanium substrata was stable enough to have sufficient capacity to combine with the carboxyl group of FN. With increased concentration of FN, the immobilized dose of FN was gradually enhanced. However, when the FN concentration was further increased, the number of the carboxyl group of FN became close to the number of the  $\text{NH}_2$  group and even beyond, which made FN immobilization tend to be stable. This might be why, when the concentration of FN increased to 300  $\mu\text{g}/\text{ml}$ , the covalently-bound FN dose was not further enhanced.

We showed that after the silanization and immobilization of FN, roughness of the smoothed titanium surfaces decreased significantly, but that of the micro-grooved titanium surfaces was not obviously influenced. This indicates that after the silanization, the generated porous structure at the nm level

remarkably decreased the roughness of smoothed surfaces, but scarcely affected that of micro-grooved surfaces, which already had relatively higher levels of roughness because of the shape of the microgrooves. The surface changes of nanoscale by the silanization had no obvious influence on the roughness at the micron scale. We also showed the hydrophilicity reflected by contact angle increased significantly in both micro-grooved and smoothed titanium substrata, probably because the  $-\text{CH}_3$  group of the titanium silane surface was replaced with the hydrophilic hydroxyl group. In addition, immobilization of FN slightly decreased the water contact angles, implying that FN functions (e.g., increasing the cell adhesion) without the cost of obviously decreasing the hydrophilicity of the titanium surface.

The HR of red blood cells is an important parameter for blood compatibility. To verify the safety of the modified implant material, we examined the HR of different surfaces. After the silanization and covalent binding of Fn, the biocompatibility of all the materials was within the normal range ( $<5\%$ ), indicating the modified titanium surfaces were safe for implantation.

We then tested the effect of modified titanium surfaces on the behaviors of HGFs, including orientation, morphology, adhesion, and proliferation. It was demonstrated that HGFs cultured on micro-grooved surfaces aligned along the grooves, a process termed contact guidance, whereas cells cultured onto smoothed titanium grew in random directions. This result was in accordance with those previously reported [17,18].

We showed that HGFs cultured on S+Fn or G+FN surfaces looked more spread out. HGFs grew along the bottom forward if cells fell into the bottom of the microgrooves, or grew forward or upward to the crest, or crossed the grooves to the other side at some depth if they fell on the sidewall. Cells on G surfaces were rarely seen growing downward into the bottom, while on G+Fn surfaces, cells were more spread out in a confluent cell layer that almost entirely covered the surface, including the bottom. On the crest, cells grew forward or crossed over edge into groove sidewalls, which was according to the distance from the edge. This result suggests that the initial cell attachment to a surface is a critical step for cell growth.

Cell adhesion is related to factors such as morphology, hydrophilic-hydrophobic property, charge, roughness, and extracellular matrix. A hydrophilic surface promotes cell adhesion. After 2 or 4 h of culturing, the number of cells with early adhesion was highest in FN-coated smoothed surfaces, probably because of their hydrophilic character. With the extension of culturing time (at 6 h), the number of adherent cells was about the same among different plates. On the other hand, cell adhesion strength on the G+FN surface was the highest during the culturing, and reached a peak earlier than that of

the other surfaces. Collectively, given the early adherent cell number and adhesion strength, it can be concluded that the G+FN surface supported the greatest cell adhesion of HGFs compared to other surfaces.

Cell adhesion plaques consist of integrins and a large number of cytoplasm-derived proteins, such as vinculin, talin,  $\alpha$ -actinin, and tensin. The cytoskeletal protein vinculin is correlated with area of adhesion plaques [19], modulating the dynamics of cell adhesions. We showed that the cytoskeleton area and expression of vinculin protein were greatest on the G+FN surfaces. Collectively, the strong cell adhesion strength achieved by G+FN surfaces might be due to: 1) the induction of the expression and secretion of cell adhesion proteins such as vinculin, 2) FN coating as an important adhesion protein, 3) more cytoskeleton area, and 4) microgrooves.

Although coating of FN on the micro-grooved or smoothed titanium surfaces enhanced the adhesion of HGFs, interestingly, compared with those cultured on S and G titanium surfaces, HGFs on S+FN and G+FN surfaces, respectively, grew more slowly. This might be related to the greater spreading of HGFs on the FN-conjugated titanium surfaces.

Surface roughness, hydrophobic character, and other factors affect the adhesion of bacteria. Consistent with the result that the roughness and hydrophilicity of the micro-grooved titanium surface were higher than those of the smoothed surface,

the bacterial *P. gingivalis* adhesion was greater in the micro-grooved titanium surfaces. Interestingly, the adhesion of *P. gingivalis* was similar between the S+FN and S titanium surfaces and between the G+FN and G surfaces, indicating that FN had no significant effect on bacterial adhesion.

## Conclusions

In comparison with the smoothed surface, micro-grooved structure (35  $\mu$ m width, 15  $\mu$ m bridge, 10  $\mu$ m depth) coated with FN guides the HGFs to align along the grooves, and promotes the spread, adhesion, and proliferation of cells. This result will be beneficial to constituting a barrier of HGFs to promote the osseointegration surrounding the implant body, which might improve the efficacy of dental implants. Further animal studies will be carried out to validate these results.

## Conflict of interest

The authors declare that they have no conflict of interest.

## Acknowledgement

We would like to thank Wego Jericom Biomaterials Co., Ltd. for helping fabricate the titanium material. This study was supported by the Key Clinical Specialty Discipline Construction Program of Fujian, P.R. China.

## References:

1. Lee HJ, Lee J, Lee JT et al: Microgrooves on titanium surface affect peri-implant cell adhesion and soft tissue sealing; An *in vitro* and *in vivo* study. *J Periodontal Implant Sci*, 2015; 45: 120–26
2. Geurs NC, Vassilopoulos PJ, Reddy MS: Soft tissue considerations in implant site development. *Oral Maxillofac Surg Clin North Am*, 2010; 22(3): 387–405, vi–vii
3. Chen X, Li Y, Aparicio C: Biofunctional coatings for dental implants. 2013
4. Iglhaut G, Becker K, Golubovic V et al: The impact of dis-/reconnection of laser microgrooved and machined implant abutments on soft- and hard-tissue healing. *Clin Oral Implants Res*, 2013; 24: 391–97
5. Lee K, Kim EH, Oh N et al: Contribution of actin filaments and microtubules to cell elongation and alignment depends on the grating depth of microgratings. *J Nanobiotechnol*, 2016; 14: 1–10
6. Lee SW, Kim SY, Lee MH et al: Influence of etched microgrooves of uniform dimension on *in vitro* responses of human gingival fibroblasts. *Clin Oral Implants Res*, 2009; 20: 458–66
7. Lee SW, Kim SY, Rhyu IC et al: Influence of microgroove dimension on cell behavior of human gingival fibroblasts cultured on titanium substrata. *Clinical Oral Implants Res*, 2009; 20: 56–66
8. Kirchhof K, Groth T: Surface modification of biomaterials to control adhesion of cells. *Clin Hemorheol Microcirc*, 2008; 39: 247–51
9. Park SJ, Leesungbok R, Ahn SJ et al: Effect of microgrooves and fibronectin conjugation on the osteoblast marker gene expression and differentiation. *J Adv Prosthodont*, 2015; 7: 496–505
10. Zhou X, Shi J, Hu J, Chen Y: Cells cultured on microgrooves with or without surface coating: Correlation between cell alignment, spreading and local membrane deformation. *Mater Sci Eng C Mater Biol Appl*, 2013; 33(2): 855–63
11. Anselme K, Bigerelle M, Noel B et al: Qualitative and quantitative study of human osteoblast adhesion on materials with various surface roughnesses. *J Biomed Mater Res*, 2000; 49: 155–66
12. Bigerelle M, Anselme K: Statistical correlation between cell adhesion and proliferation on biocompatible metallic materials. *J Biomed Mater Res Part A*, 2005; 72A: 36–46
13. Bagno A, Piovan A, Dettin M et al: Improvement of Anselme's adhesion model for evaluating human osteoblast response to peptide-grafted titanium surfaces. *Bone*, 2007; 41: 704–12
14. Kaiser JP, Reinmann A, Bruinink A: The effect of topographic characteristics on cell migration velocity. *Biomaterials*, 2006; 27: 5230–41
15. Lee SW, Kim SY, Lee KW: Surface microgrooves of thirty micrometers in width on titanium substrata enhance proliferation and alter gene expression of cultured human gingival fibroblasts. *J Korean Acad Prosthodont*, 2007; 45(6): 787–94
16. Clark P, Connolly P, Curtis AS et al: Topographical control of cell behaviour. I. Simple step cues. *Development*, 1987; 99: 439–48
17. Meyle J, Gültig K, Wolburg H, Von Recum AF: Fibroblast anchorage to microtextured surfaces. *J Biomed Mater Res*, 1993; 27: 1553–57
18. Walboomers XF, Ginsel LA, Jansen JA: Early spreading events of fibroblasts on microgrooved substrates. *J Biomed Mater Res*, 2000; 51: 529–34
19. Hunter A, Archer CW, Walker PS, Blunn GW: Attachment and proliferation of osteoblasts and fibroblasts on biomaterials for orthopaedic use. *Biomaterials*, 1995; 16: 287–95